DOI: 10.3901/CJME.2015.0316.059, available online at www.springerlink.com; www.cjmenet.com; www.cjme.com.cn

Three-dimensional Construction and Omni-directional Rolling Analysis of a Novel Frame-like Lattice Modular Robot

DING Wan, WU Jianxu, and YAO Yan'an*

School of Mechanical, Electronic and Control Engineering, Beijing Jiaotong University, Beijing 100044, China

Received September 18, 2014; revised March 2, 2015; accepted March 16, 2015

Abstract: Lattice modular robots possess diversity actuation methods, such as electric telescopic rod, gear rack, magnet, robot arm, etc. The researches on lattice modular robots mainly focus on their hardware descriptions and reconfiguration algorithms. Meanwhile, their design architectures and actuation methods perform slow telescopic and moving speeds, relative low actuation force verse weight ratio, and without internal space to carry objects. To improve the mechanical performance and reveal the locomotion and reconfiguration binary essences of the lattice modular robots, a novel cube-shaped, frame-like, pneumatic-based reconfigurable robot module called pneumatic expandable cube(PE-Cube) is proposed. The three-dimensional(3D) expanding construction and omni-directional rolling analysis of the constructed robots are the main focuses. The PE-Cube with three degrees of freedom(DoFs) is assembled by replacing the twelve edges of a cube with pneumatic cylinders. The proposed symmetric construction condition makes the constructed robots possess the same properties in each supporting state, and a binary control strategy cooperated with binary actuator(pneumatic cylinder) is directly adopted to control the PE-Cube. Taking an eight PE-Cube modules' construction as example, its dynamic rolling simulation, static rolling condition, and turning gait are illustrated and discussed. To testify telescopic synchronization, respond speed, locomotion feasibility, and repeatability and reliability of hardware system, an experimental pneumatic-based robotic system is built and the rolling and turning experiments of the eight PE-Cube modules' construction are carried out. As an extension, the locomotion feasibility of a thirty-two PE-Cube modules' construction is analyzed and proved, including dynamic rolling simulation, static rolling condition, and dynamic analysis in free tipping process. The proposed PE-Cube module, construction method, and locomotion analysis enrich the family of the lattice modular robot and provide the instruction to design the lattice modular robot.

Keywords: modular robot, pneumatic expandable cube, pneumatic actuation, omni-directional rolling, binary control strategy

1 Introduction

Terrestrial mobile robots mainly include wheeled, tracked, legged, hybrid, snake, and spherical robots[1–2]. Even though each configuration type has its unique adaptability, and locomotion modes, a constant structure can't adapt to comprehensive complex environments and execute the requirements of multiple functions and tasks[3–4]. Reconfigurable robots consisted of multiple identical or different functional building blocks have the capability to adapt to the operating environment and multiple tasks by reconfiguring their own structure and configuration[5]. They can be normally classified into three architectural types that are chain, lattice, and mobile reconfigurations[6]. Generally, the chain and lattice architectures are more commonly explored. The chain types possess the serial structures, like string or tree topology, of which structures perform more versatile, such as, legged walking, ring-shape rolling, snake-like crawling, serial manipulator's operating, etc[7–8]. However, the chain types are more difficult to control and analyze; compared with chain types, although lattice types compromise mobility, they can be controlled more easily due to their simpler reconfiguration strategy[9]. And, modules must be arranged and reconfigured to certain neighboring positions. Such motion is essentially a binary process; meanwhile, the motion can be realized by using binary signal(0/1) to control the robot[10]. As shown in Fig. 1, taking cubic lattice module as example, two reconfiguration modes including translation and rotation are illustrated. Each mode possesses four possible target positions in one step, of which positions the moving module must reach.

For the lattice types, most of researches mainly focus on hardware descriptions and reconfigurable algorithms of the proposed modules. Few of them discuss and analyze the locomotion modes in certain configuration[11]. And also, due to their hardware design and actuation methods, the locomotion speed and actuation force output are relatively low, and they don't have any internal space to carry objects.

* Corresponding author. E-mail: yayao@bjtu.edu.cn

Supported by National Natural Science Foundation of China(Grant No. 51175030), Fundamental Research Funds for the Central Universities, China(Grant No. 2012JBZ002), Research Fund for the Doctoral Program of Higher Education(Grant No. 20130009110030), and Major Project of Ministry of Education of China(Grant No. 625010403)

© Chinese Mechanical Engineering Society and Springer-Verlag Berlin Heidelberg 2015

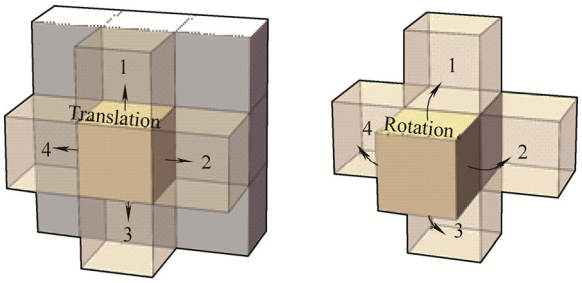

(a) Translation reconfiguration (b) Rotation reconfiguration

Fig. 1. Two reconfiguration modes of lattice modular robot

For the lattice modular robots, the actuation methods are diversity. One method is directly actuated by electric telescopic rod. BUTLER, et al[12–13], developed two version prototypes of self-reconfigurable compressible modules called Crystalline Atom, and the peristalsis motion was illustrated. SUH, et al[14], presented a self-reconfigurable modular robot called Telecube, which telescopes its six faces out independently by six special designed telescopic rods. WELLER, et al[15], designed a Prismatic Cube Module with the same structure as Telecube to verify the proposed algorithms and show the hardware demonstration. KARAGOZLER, et al [16], designed an electrostatic-based modular robot to describe the macroscale electrostatic latch. YU, et al[17], presented a self-deformable modular robot called Morpho, which mainly illustrated the construction concept and several deformation configurations. YU, et al [18], assembled a pressure-adaptive cubic modular column that can adjust its configuration according to pressure position. The second method takes advantage of robot arms to reconfigure. UNSAL, et al[19], and PREVAS, et al[20], proposed a class of 3-D module called I-Cubes with an active moving link to reconfigure, which mainly described the hardware and reconfiguration algorithm. HJELLE, et al [21], addressed a concept of robotically reconfigurable truss that reconfigures itself by adopting robot arms moving on the attachable linkage. The rest methods are indirectly actuation, such as magnet, gear rack, flywheel, etc. AN, et al[22], adopted permanent magnets and electromagnets to develop and actuate an EM-Cube with sliding motion among modules. MICHAEL[23] used the pinion and rack to create a polymorphic robot called Fractal robot. ROMANISHIN, et al[24], developed a cubic modular robot without exterior available space called M-Blocks which moves by adopting its built-in flywheel to provide the angular momentum of locomotion.

By considering constructing a module with large internal space, the frame-like structure can be regarded as an ideal choice. AGRAWAL, et al[25], provided a way to construct a single DoF expanding structures by adopting polyhedral expanding building blocks, like tetrahedron, cube, etc. CLARK, et al[26], and CURTIS[27] proposed a modular design concept of planetary exploring robots by only using electric telescopic rods and node components as building blocks to construct frame-like robots with payloads carried in the center, such as 4-TET (Tetrahedron) and 12-TET.

In our previous work[28], a pneumatic-based mobile mechanism constructed by only prismatic joints was studied. The experiments showed that the pneumatic system performed good reliability and repeatability, and that the lightweight mini aluminium alloy(MAL) pneumatic cylinder performed high output-weight ratio, telescopic synchronization, stiffness, and telescopic and responding speed. The potential binary control strategy cooperated with binary actuator(pneumatic cylinder) made the mechanism easy to control. And also, the simple construction, redundant actuation, capability of absorbing shock provided good design references.

Since the reconfiguration process of the lattice modular robots is essentially a binary process, we try to extend the binary process to control locomotion, and to integrate the above characteristics to enhance mobility. Therefore, the concept of only prismatic joints construction, binary control strategy, and pneumatic system are directly adopted to create a novel lattice reconfigurable modular robot called PE-Cube. The PE-Cube is reconfigured and disassembled by human operator. The hardware description, way of constructing symmetric 3-D structures, and rolling locomotion analysis and experiments of the constructed robots are the main focuses.

The paper is organized as follows. Section 2 illustrates the construction, control, and expansion of the PE-Cube modules. Section 3 analyzes the static rolling condition and locomotion gaits of eight PE-Cube modules' construction. Section 4 describes the experimental pneumatic-based robotic system and carries out the experiments. Section 5 simulates the dynamic rolling of the thirty-two PE-Cubes' construction and analyses its static rolling condition and gait.

2 PE-Cube Construction and Expansion

The construction description and potential binary control strategy of the PE-Cube are described. The connection and expansion methods between two PE-Cube modules are presented. And, the construction condition of assembling the completely symmetric 3-D structure is depicted.

2.1 Construction description

As shown in Fig. 2(a), a sketch diagram, a PE-Cube with eight links($Link_1$ to $Link_8$) and twelve prismatic joints(P_1 to P_{12}) is shaped by replacing each edge of a geometry cube with reversibly deployable strut consisted of a piston and a sleeve. As displayed in Fig. 2(b), the PE-Cube includes two kinds of vertex components that are piston component (three meeting pistons) and sleeve component(three meeting sleeves). Fig. 2(c) is the prototype composed of twelve MAL pneumatic cylinders and eight connecting cubic blocks.

The DoF(F) of the cube unit is calculated by modified Grübler- Kutzbach criterion[29–31]:

$$F = d(n-g-1)+\sum_{i=1}^{g} f_i + v - \zeta, \tag{1}$$

where λ is the number of independent common constraints in the mechanism, d=6–λ is called order of the mechanism, n is the total number of links, g is the number of kinematic pairs, f_i is the DoF of the ith kinematic pair, v represents the number of redundant constrains, and ζ is the passive DoF.

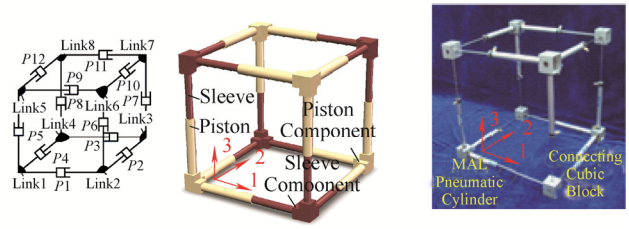

(a) Sketch diagram (b) 3D module (c) Prototype

Fig. 2. PE-Cube module

According to the screw system, the common constraint of the inner cube is three due to the only prismatic joints construction(refer to Ref. [28] for an example of the construction). In this work, by using λ=3, d=3, n=8, g=12, f_i=12, v=2×9–3×4=6, ζ=0, the DoF of the mechanism is F=3 according to Eq. (1). Its three independent telescopic directions are shown in Fig. 1(b) and Fig. 1(c). It needs to expand four pneumatic cylinders simultaneously for each independent DoF.

2.2 Binary control strategy

Generally, the binary manipulator is actuated by two-state actuator called binary actuator[32–33]. Binary means the value of the variable has only one of two states(0/1). The MAL pneumatic cylinder with two extreme states('min/max' length) is an ideal binary actuator. Due to redundant actuation of each DoF, four parallel prismatic joints are actuated simultaneously by giving a binary signal 0/1. The numbers 0 and 1 represent the shortest and longest lengths, respectively. See Fig. 3, eight possible configurations and their corresponding binary codes of a PE-Cube are described. Therefore, this control process is called binary control strategy.

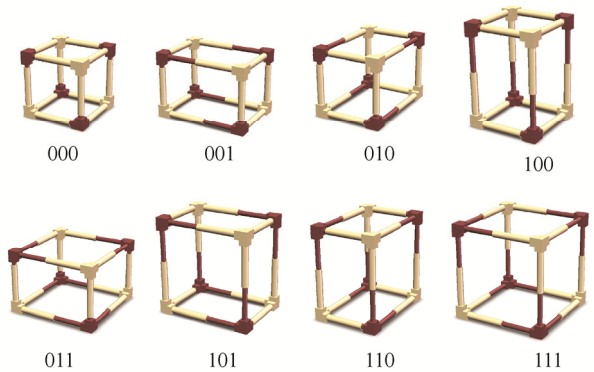

Fig. 3. Eight possible configurations of a PE-Cube

2.3 Connection and expansion

As depicted in Fig. 4, there are four possible connection methods(five positions) between two PE-Cubes. The lock represents that the neighboring two vertex components (piston or sleeve component) are fixed. The four possible connection methods are as follows: 1) position 1; 2) position 2 or 3; 3) positions 2 and 3; 4) positions 2, 3, 4 and 5. The different connection methods will cause partial coupling and decoupling between two modules. The n cubes combination(where n is the number of cubes) are described as n-Cube for short. Here, "combination" means the modules are only put together without being connected, while, "construction" means the modules are combined and connected together.

Fig. 4. Connection methods between neighboring two PE-Cubes

As shown in Table 1, the constructed 3-D configurations and their 2-D projections on the symmetry plane are displayed. The configurations are set and selected as the completely symmetric 3-D structure. The configurations are classified according to the number of cubes that are projected on the symmetry plane(⩽12-Cube). Each of them has three principal axes that are the axis of symmetry of the configuration and pass through its geometry center(x-, y-, z-axis)[34]. And, they satisfy 90 and 180 degrees rotation symmetry. Due to limited space, the cubes along each principle axis are prescribed less than or equal to four.

Table 1. Combinations of 4-, 5-, 8-, 9- and 12-Cube

4-Cube	5-Cube	8-Cube	9-Cube	12-Cube
	9-Cube	12-Cube		32-Cube (I)
8-Cube	6-Cube	20-Cube	27-Cube	32-Cube (II)

The symmetry structure makes the constructed robots possess the same properties when each surface of the constructed configuration touches the ground. In the following sections, the locomotion properties of two 3-D

configurations that are 8-Cube and 32-Cube(I) will be selected as examples to discuss and analyze their locomotion properties.

3 Eight-Cube Construction

The omni-directional locomotion feasibility of 8-Cube construction is analyzed and verified in this part. It includes construction description, dynamic simulation, static tipping condition analysis, experimental hardware system description, and rolling and turning motion experiments.

3.1 Structure description

As displayed in Fig. 5(a), eight modules are connected to form the 8-Cube construction by fixing eight meeting piston components located at its geometry center. The connection position between two modules can be position 1 or 2 shown in Fig. 4. Thus, each PE-Cube can realize locomotion of expansion and contraction independently. Fig. 5(b) illustrates the symmetry plane and the projection profile of the 8-Cube construction.

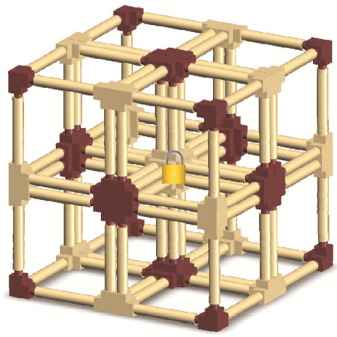

(a) 3-D model and its connection

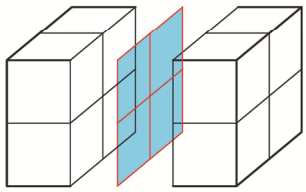

(b) Symmetry plane and its projection profile

Fig. 5. Connection of the 8-Cube construction

3.2 Dynamic simulation

As shown in Fig. 6, a period of dynamic tipping motion is simulated by using the commercial dynamic software ADAMS™ as the extension ratio equals to 1.54. Here, the extension ratio 1.54 is the value of the selected standard MAL pneumatic cylinder. According to tipping gait planning, the whole process is divided into four steps.

The expansion speed at the third step is set as 50 mm/s. After four steps, the robot goes back to its initial state, and all expanded struts are contracted to original length. Then, a period of tipping gait is achieved, and the robot moves a distance forward. By repeating the tipping gait, the robot can realize rolling along a straight line.

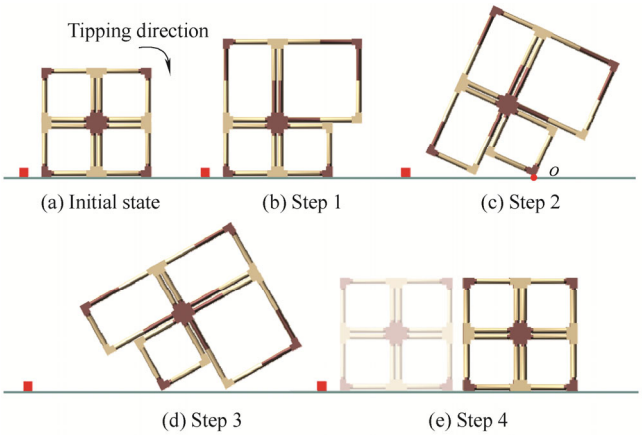

Fig. 6. Screen-captures of a period of tipping gait

3.3 Static tipping analysis

According to the dynamic tipping simulation, we know that the second and third steps are the critical steps of tipping. By considering the statically stable locomotion, the stability of the robot only has relations with its geometry shape[35]. The stability only needs to judge whether the projection of the center of mass(CM) of the robot locates in the supporting region. Thus, the static tipping analysis that has only relations with the extension ratio of each deployable strut is carried out to judge the stability[28].

As the extension ratio μ increases from 1.3 to 1.85, the CM variation of the second and third steps is shown in Fig. 7. The critical edge represents the rotation axis that passes through axis o and is vertical to the paper plane . From Fig. 7, we can infer that the robot reaches its critical condition of tipping at the second step as the extension ratio μ=1.82. Once the extension ratio continuously increases, the projection point of the CM will exceed the rotation axis o, and the robot will rotate around axis o. What's more, the mechanism is stable during the rest steps as the extension ratio increases from 1.3 to 1.85. That is to say, the robot can achieve static tipping.

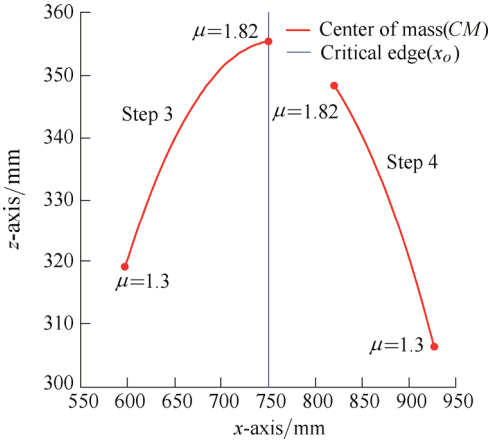

Fig. 7. Extension ratio and stability analysis

Therefore, the two critical steps with its CM position and projection are displayed in Fig. 8 as the extension ratio μ=1.82. As shown in Fig. 8(a), the robot reaches the critical condition of tipping. As displayed in Fig. 8(b), the CM projection locates in the stable region.

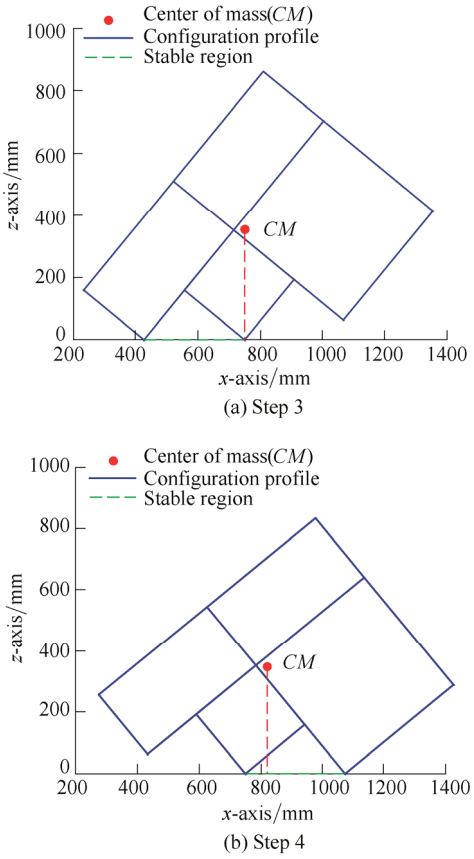

Fig. 8. Statically stable analysis

3.4 Turning locomotion description

As shown in Fig. 9, a new gait is illustrated. The robot can turn an angle by taking advantage of the friction couple caused by the unevenly distribution of the normal force. By lifting up the cube at the fifth step, the equally distribution of the normal forces is broken. We get that the normal force of point C is larger than the sum of the normal force of the points A, D and E as two cubes contract at the sixth step, which is demonstrated by measuring the friction in the ADAMS™. Hence, the different values of the kinetic frictions generate a torque of the friction couple to make a robot turn an angle.

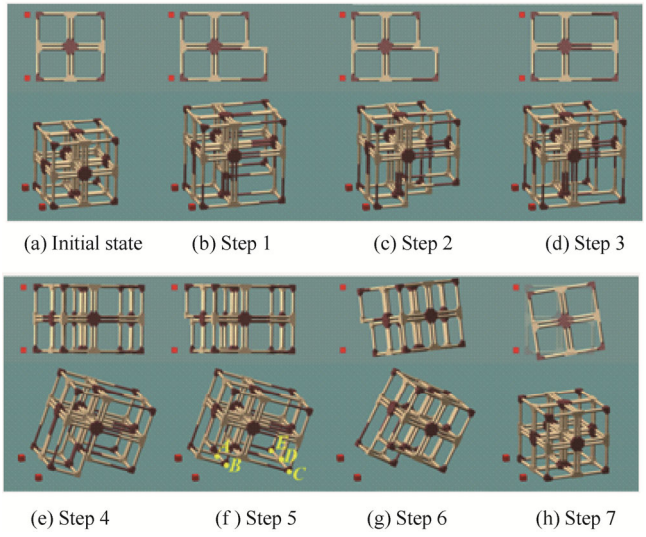

Fig. 9. Screen-captures of a turning locomotion simulation

Here, the turning motion provides other constructed robots with a more efficient way to select the motion directions rather than turning by synthesizing two directions together like feed movement.

By synthesizing the rolling and turning motion, the robot can realize omni-directional locomotion. The locomotion paths are shown in Fig. 10. In the tipping gait, the robot can tip into four possible regions(see path I). What's more, the robot can move in more directions after excuting the turning motion(see Paths II and III).

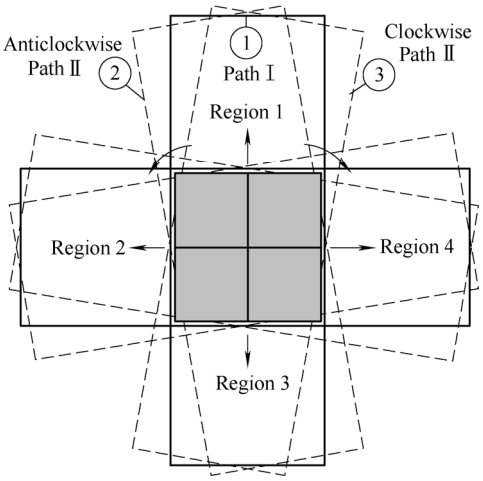

Fig. 10. Locomotion paths

4 Experimental Pneumatic-Based Robotic System and Experiments

4.1 Hardware description

As shown in Fig. 11, an experimental pneumatic-based robotic system composed of PE-Cubes, pneumatic system, a control unit, wireless units, a computer and a power supply is built(see Table. 2 for a summary of the specifications for the pneumatic system). Two PE-Cube modules represent the completely contracted and expanded states, respectively. And, the computer is used to transfer the binary codes to the control unit by adopting wireless unit. The control unit is designed to receive the commands and control the electric solenoid valves. The air compressor with a compressed air storage tank provides sustaining 0.7MPa air flow, and it cooperates with electric solenoid valves to control the expanding or contracting state of the pneumatic cylinder. The power supply device is used to provide a working voltage of 24 V.

In order to show the detailed construction of a PE-Cube module, the mechanical components and their connection relations of a PE-Cube are depicted in Fig. 11. The mechanical components include connecting cubic block, angle aluminiums(ϕ6 and ϕ16), connecting link, MAL pneumatic cylinder, washers, nuts, and bolts.

The cubic connecting block is a thin-wall cubic shell without up and bottom covers, which possesses two ϕ6 and two ϕ16 through-holes. One angle aluminum has two ϕ6 through-holes at the center of the two sides so as to connect

the piston; the other angle aluminum has two ϕ16 through-holes used to connect the sleeve. Cubic connector is formed by embedding an angle aluminum into the cubic connecting block and connecting them by another pneumatic cylinder. As illustrated on the bottom right of Fig. 11, the connected vertex components of two PE-Cubes shown in Fig. 4 are fixed by connecting two pneumatic cylinders with connecting links and connecting cubic blocks with bolted connection. According to Table 2, the maximum force of each pneumatic cylinder in expansion and contraction processes are 14.07 kg and 12.09kg respectively as the input pressure maintains 0.7MPa. Theoretically, one pneumatic cylinder can lift five PE-Cubes at a time in an expansion process.

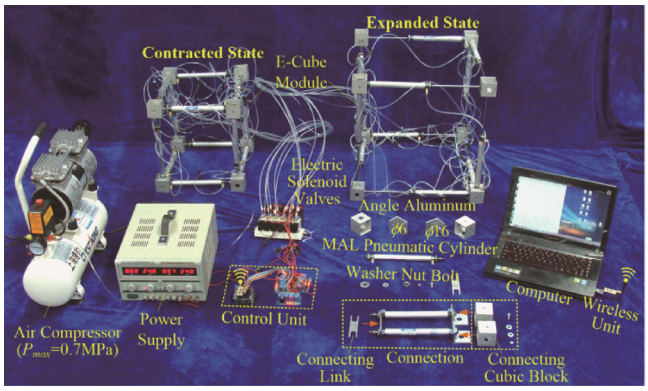

Fig. 11 Experimental pneumatic-based robotic system

Table 2. Summary of the specifications for the pneumatic system

Item	Parameter		Value
MAL pneumatic cylinder	Inner bore/mm		16
	Original length/mm		257
	Standard stroke/mm		150
	Weight/kg		0.15
	Operating speed range(mm • s^{-1})		30–800
	Stressed area/cm^2	Expanded	2.010
		Contracted	1.727
	Fluid		Air
	Pressure range/MPa		0.1–0.9
	Pressure-proof/MPa		1.35
Air compressor	Air flow/(L • min^{-1}) /Volume/L		40/8
	Maximum pressure/MPa		0.7
	Voltage/V/Frequency/Hz		220/50
PE-cube module	Mass/kg		2.7
	Extension ratio		1.54
	Module size /(mm×mm×mm)	Minimum (contracted)	280×280×280
		Maximum (expanded)	430×430×430

4.2 Tipping and Turning Locomotion Experiments

As displayed in Figs. 12 and 13, the tipping and turning locomotion experiments of the 8-Cube robot are carried out to validate the feasibility of the experimental robotic system and its locomotion gaits. For the 8-Cube robot, a two dimensional array A[8][3] with 24 elements is used to control the robot. Such as, the value of the array A[8][3] ={000; 000; 000; 000; 000; 000; 000; 000;} represents all the pneumatic cylinders of the robot are contracted. The telescopic state and direction of each PE-Cube is described as A[n][3]={n-x n-y n-z} (where n is the sequence of cubes, n=1, 2,⋯, 8; x, y and z represent the telescopic direction; n-x/n-y/n-z equal 0/1).

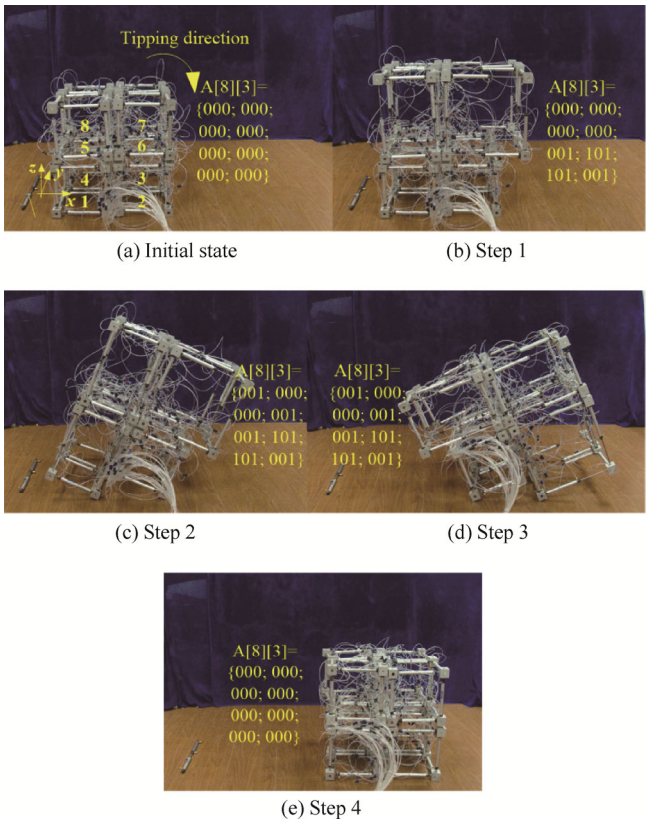

(a) Initial state (b) Step 1

(c) Step 2 (d) Step 3

(e) Step 4

Fig. 12 Tipping locomotion experiment

5 32-Cube Construction

5.1 Structure analysis

The 32-Cube omni-directional rolling robot is constructed by connecting the corresponding parts of 32 PE-Cubes as depicted in Fig. 14(a). The adjacent two PE-Cubes are connected by connection method (2). There are totally 20 connected positions. In Fig. 14(a), the four cubes meeting at the each corner are connected by fixing the common vertex components at position 1. And, the two cubes on each edge are connected at position 2. Extracting the twelve edges connected by the vertex components, we can get a closed-loop inner cube as displayed in Fig. 14(b).

By using d=3, λ=3, n=20, g=24, f_i=24, v=v=2×6−3×2=6, ζ=0, the DoF of the mechanism is 15 according to Eq. (1). There are totally three groups of parallel edges of a PE-Cube. For the inner cube, by choosing any one of the three groups of parallel edges, we can find that one of its four parallel edges must mount two active actuators, and, the rest of each edge should allocate one active actuator. There are three passive movements in each group. We can easily get that the DoF of the PE-Cube mounted at eight corners respectively is three and the DoF of the rest

PE-Cubes are two without considering the DoF of the inner cube. So, the number of active actuators can be calculated as $F=3\times8+2\times12\times2+15=87$.

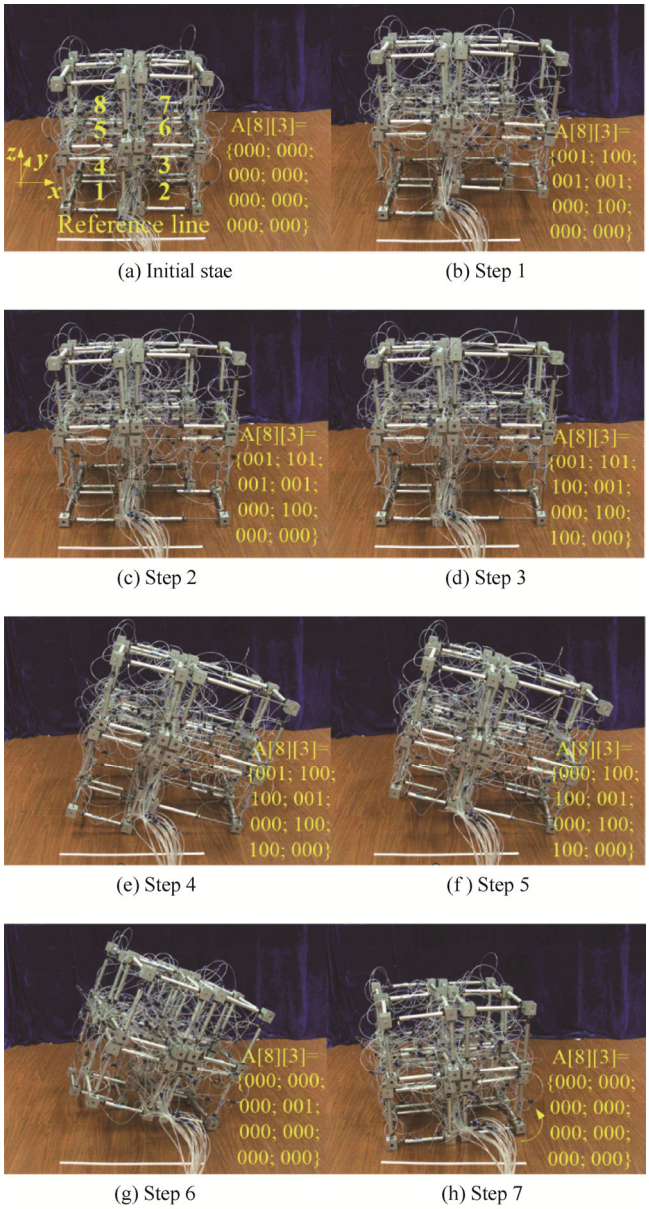

(a) Initial stae (b) Step 1

(c) Step 2 (d) Step 3

(e) Step 4 (f) Step 5

(g) Step 6 (h) Step 7

Fig. 13 Turning locomotion experiment

5.2 Dynamic Simulation

See Fig. 15, the dynamic rolling simulation of the robot is divided into seven steps. The execution of each step should satisfy the rotation condition that the projection of the CM of the step i must exceed the rotation axis o_{i-1} (i=2, 3, 4, 5). The extension ratio μ and telescopic speed v are set to 1.54 and 200 mm/s, respectively. According to the symmetry of the construction, the robot can realize omni-directional locomotion like 8-Cube construction.

5.3 Tipping Analysis

In this part, we mainly focus on calculating the extension ratio that satisfies the static tipping condition. The mathematic model of the 32-Cube can refer to the process analyzed in Ref. [28]. Suppose that the initial extension ratio equals to 1.2. If the extension ratio cannot satisfy the required condition for executing the next step, the extension ratio will add 0.01 and repeat previous steps from the beginning of the locomotion, which is called iteration process(*IP*). The steps 1 to 3 displayed in Fig. 15(b), (d) and(e) are called self-deformation processes(*SP*) 1 to 3, respectively.

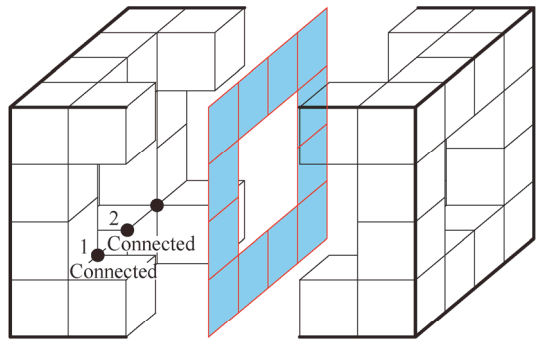

(a) Connected part and symmetry plane

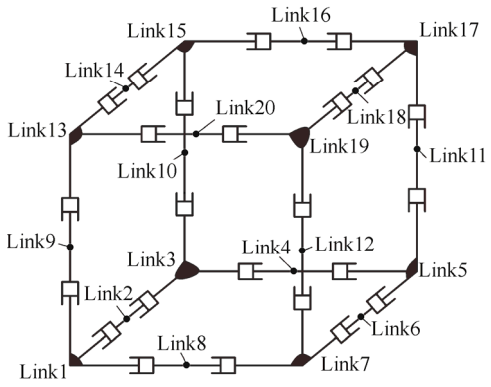

(b) Sketch diagram of the inner cube

Fig. 14 Connection of the 8-Cube Combination

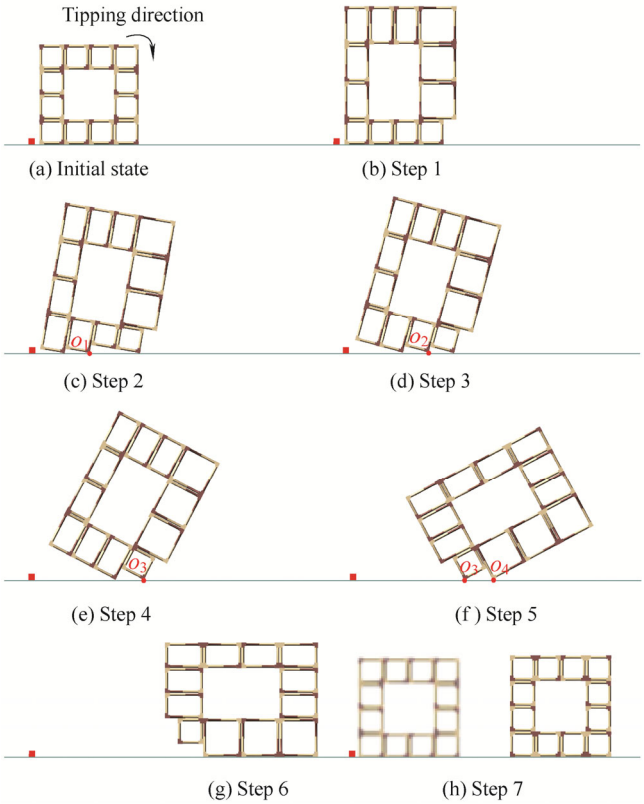

(a) Initial state (b) Step 1

(c) Step 2 (d) Step 3

(e) Step 4 (f) Step 5

(g) Step 6 (h) Step 7

Fig. 15. Screen-captures of a period of tipping gait

Coordinate of the CM with respect to the different extension ratios at the end of each step in the whole iteration process is plotted in Fig. 16. The trajectory can be divided into two categories, namely, three self-deformation processes(*SP*1, *SP*2 and *SP*3) without considering the step 2 and four iteration processes(*IP*11, *IP*12, *IP*21, *IP*22).

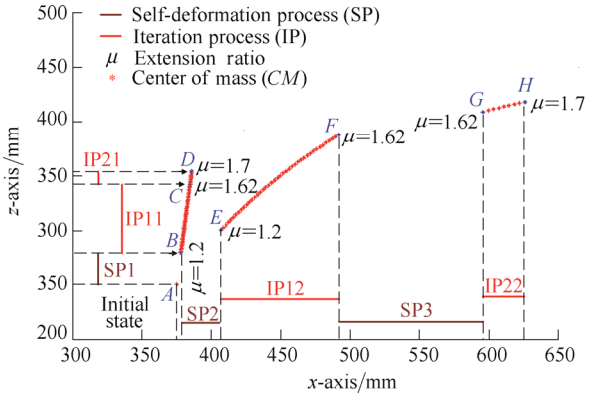

Fig. 16. Trajectory of the CM with different extension ratios

When the mechanism is at its initial state, the *CM* is at point *A*. After the first self-deformation process(*SP*1) at the step 1, the *CM* translates to point *B* as extension ratio equals to 1.2. The *SP*2 that corresponds to the steps 2 and 3 moves the CM to point *E*. Because this extension ratio cannot satisfy the required condition for executing the step 3, then, the extension ratio adds 0.01 and the mechanism repeats the former three steps(*IP*11 to *IP*12) to meet the condition. After forty-three iterations, the *IP*12 stops as the extension ratio equals to 1.62. The *SP*3 that corresponds to the step 4 moves the CM to the point *G* as the extension ratio 1.62. By increasing the extension ratio in following nine times of iterations, the require condition of the step 5 is satisfied as the extension ratio equals to 1.7 at point *H*. In *IP*21 to *IP*22, the CM coordinates calculated at the step 3 are not shown in Fig. 16 for clearity.

From the forth step (Fig. 14(e)) to the fifth step (Fig. 15(f)) is a freely tipping process. It's a dynamic tipping process. Fig. 17(a) shows that the *CM* projection of the robot at the fifth step, which represents that the robot is stable without considering the moment of inertia. Thus, the zero-moment-point(ZMP) analysis of the mechanism is adopted to analysis the stability of the robot in the free tipping phase. For biped robot, ZMP analysis is used to judge the dynamic balance in the motion process[36–37]. ZMP that is regarded as the center of pressure at the supporting surface located on the ground is a point where the resultant moment is zero[38]. The condition of stable locomotion can be described as following ZMP criterion: the ZMP of the robot must locate in the supporting area. ZMP can be represented as follows:

$$x_{\mathrm{ZMP}}=\frac{\sum_{i=0}^{n}m_i(\ddot{z}_i+g_z)x_i-\sum_{i=0}^{n}m_i\ddot{x}_iz_i-\left(\sum_{i=0}^{n}J_i\alpha_i\right)_y}{\sum_{i=0}^{n}m_i(\ddot{z}_i+g_z)},\quad(2)$$

where m_i are the masses of link i, x_i , y_i and z_i are the positions of the center of mass of link i, $\ddot{x}_i$, $\ddot{y}_i$ and $\ddot{z}_i$ are the accelerations along the x-axis, y-axis, and z-axis respectively, g_z is the gravitational acceleration which equals to 9.8 $\mathrm{m/s^2}$, J_i and α_i are the moment of inertia and angular acceleration of the ith link. See Fig. 17(b), the robot is rolling along the positive x-axis.

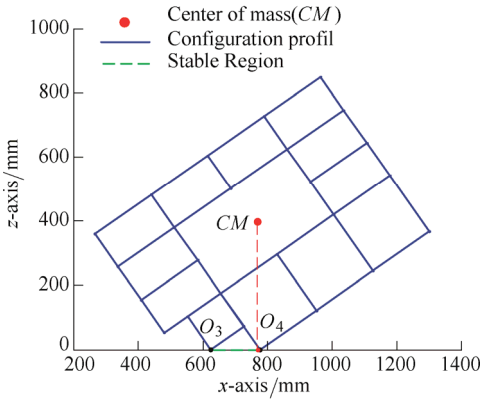

(a) Configuration profile of step 5

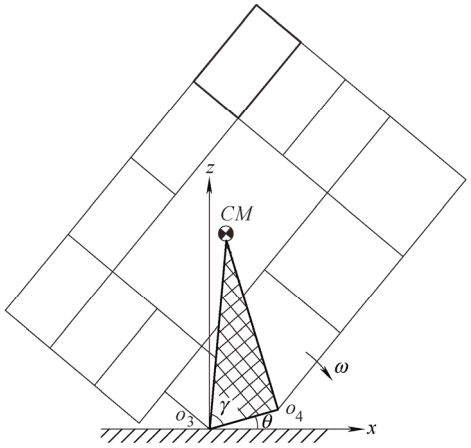

(b) Simplified model of free tip process

Fig. 17. Stability analysis of step 5

Different from the dynamic stable locomotion, we try to control the ZMP of the robot to move out of the supporting area to achieve tipping[39]. After step 4, the robot will tip freely and rotate around the vertex o_3. During its freely tipping process caused by the gravity, the stability of the robot at the end of the fifth step is analyzed. See Fig. 17(b), the coordinate frame o_3-xz is built and the vertex o_3 is the original point. The *CM* position of the robot and the angle γ can be computed from Eqs. (3) and (4), respectively. The mass of the robot is M. The mass of each deployable strut equals to m. The freely tipping angle θ_0 is calculated by Eq. (5). Deriving the second derivative of the *CM*, the accelerations along the x-, y-, and z-axis are expressed in Eq. (6):

$$CM=\begin{pmatrix}\|CMo_3\|\cos(\gamma+\theta)\\0\\\|CMo_3\|\sin(\gamma+\theta)\end{pmatrix},\quad(3)$$

$$\gamma = \arccos\left(\frac{\|CMo_3\|^2 + \|o_3o_4\|^2 - \|CMo_4\|^2}{2\|o_3o_4\| \cdot \|CMo_4\|}\right), \tag{4}$$

$$\theta_0 = \arctan(\mu - 1), \tag{5}$$

$$\ddot{CM} = \begin{pmatrix} -\|CMo_3\|\left(\alpha \sin(\gamma+\theta) - \omega^2 \cos(\gamma+\theta)\right) \\ 0 \\ \|CMo_3\|\left(\alpha \cos(\gamma+\theta) + \omega^2 \sin(\gamma+\theta)\right) \end{pmatrix}. \tag{6}$$

According to the Parallel Axis Theorem, the moment of inertia J_{o_3} of the robot rotating around the axis that passes through vertex o_3 and parallels to y-axis is calculated as

$$J_{o_3} = \frac{1}{3} m l_0^2 \left(463\mu^2 + 180\mu + 909\right), \tag{7}$$

where ||*|| denotes the distance between two points, m is the mass of each strut of a PE-Cube, l_0 is the original length of each strut, μ is the extension ratio.

By applying the Newton's Second Low for rotation, we can get the angular acceleration α as

$$\alpha = \frac{Mg\|CMo_3\|\left[\cos(\gamma+\theta) - \cos(\gamma+\theta_0)\right]}{J_{o_3}}. \tag{8}$$

Then, by changing the variables and using integration, the angular velocity ω can be calculated as

$$\omega = -\sqrt{\frac{2Mg\|o_3o_4\|(\sin\theta_0 - \sin\theta)}{J_{o_3}}}. \tag{9}$$

According to Eqs. (3) to (9), the ZMP function is expressed as

$$x_{\text{ZMP}} = \frac{M(C\ddot{M}_z + g)CM_x - MC\ddot{M}_x CM_z - J_{o_3}\alpha}{M(C\ddot{M}_z + g)}. \tag{10}$$

For the robot shown in Fig. 17, the stable region along the X-axis is o_3o_4. As X_{zmp} moves out of the stable region, the mechanism will tip. Therefore, at the rotation direction, the tipping condition can be judged as

$$x_{\text{ZMP}} > \|o_3o_4\|. \tag{11}$$

Using the value of the parameters displayed in Table. 3, we can get the x_{ZMP} in the free tipping process. See Fig. 18, the stable region is o_3o_4 and the x_{ZMP} exceeds this region when θ decreases to 0.25(rad). Therefore, the robot directly tips around axis o_4.

Table 3. The value of the parameters

μ	l_0/mm	m/kg	M/kg	g/(m • s^{-2})
1.7	250	0.15	57.6	9.8
$\|CMo_4\|$/mm)	$\|CMo_4\|$/mm)	$\|o_3o_4\|$/mm	γ/rad	θ_0/rad
836.13	785.25	305.16	1.22	0.35

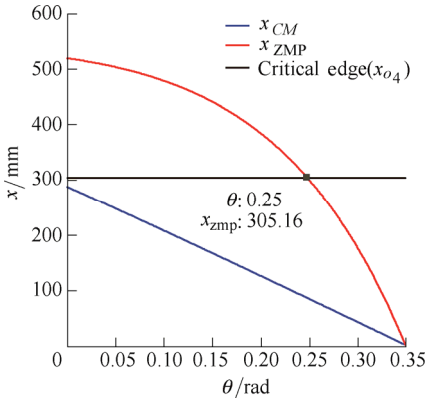

Fig. 18. Trajectory of x_{zmp} and x_{CM} with respect to θ

According to the analysis mentioned above, the robot can achieve the tipping motion as the extension ratio equals to 1.7. As shown in Fig. 19, the trajectory of the CM in a period of tipping motion from the initial state to the step 7 is displayed.

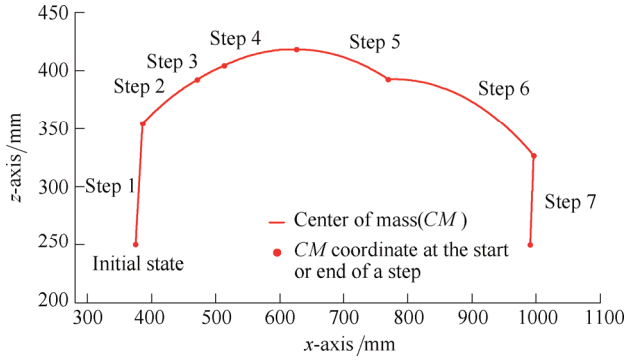

Fig. 19. Trajectory of the CM in a period of tipping motion

6 Conclusions

(1) The PE-Cube lattice reconfigurable modular robot adopts frame-like structure to create large available internal space that can carry payloads. The binary actuator is used directly to reveal the binary essence of lattice reconfigurable modular robot. The PE-Cube is only composed of mainly two components that are pneumatic cylinder and connecting cubic block.

(2) The practical prototype experiments of the rolling and turning gaits of the 8-Cube construction together with the dynamic simulations testify the feasibility and validity of the modular design concept and its locomotion properties. The numerous experiments verified the reliability and repeatability of the experimental pneumatic-

based robotic system. And, each module is testified to have high telescopic synchronization, which has small influence caused by the cylinder friction. The expanded pneumatic cylinder plays an importance role in absorbing the shock in tipping gait. The usage of the binary control strategy reduces the complexity of the programming and instruction codes of wireless communication, which made the robot easy to control.

(3) As a new member of the lattice reconfigurable modular robot, the frame-like structure and pneumatic actuation with small extension ratio, high telescopic and response speed, the large actuation strength, lightweight, small size and binary property provide the references for studying the lattice robot. After integrating the power system into each module and designing the robot with self-configuration function in the next step, it'll prospectively have stronger capabilities to cope with changing environments.

References

[1] BRUZZONE L, QUAGLIA G. Review article: locomotion systems for ground mobile robots in unstructured environments[J]. *Mechanical Sciences*, 2012, 3(2): 49–62.

[2] LIU J, WANG Y, LI B, et al. Current research, key performances and future development of search and rescue robot[J]. *Chinese Journal of Mechanical Engineering*, 2006, 42(12): 1–12. (in Chinese)

[3] YIM M, DUFF D G, ROUFAS K. Modular reconfigurable robots, an approach to urban search and rescue[C]//*1st International Workshop on Human-friendly Welfare Robotics Systems*, 2000: 69–76.

[4] DUAN X, HUANG Q, XU Y. Development and motion analysis of miniature wheel-track-legged mobile robot[J]. *Chinese Journal of Mechanical Engineering(English Edition)*, 2007, 20(3): 24–28.

[5] YIM M, WHITE P, PARK M, et al. *Modular self-reconfigurable robots*[M]. Springer New York: Encyclopedia of Complexity and Systems Science, 2009: 5618–5631.

[6] YIM M, ZHAGN Y, DUFF D. Modular robots[J]. *Spectrum*, 2002, 39(2): 30–34.

[7] MURATA S, YOSHIDA E, KAMIMURA A, et al. M-TRAN: Self-reconfigurable modular robotic system[J]. *IEEE/ASME Transactions on Mechatronics*, 2002, 7(4): 431–441.

[8] YOSHIDA E, MATURA S, KAMIMURA A, et al. A self-reconfigurable modular robot: reconfiguration planning and experiments[J]. *The International Journal of Robotics Research*, 2002, 21(10–11): 903–915.

[9] YIM M, SHEN W M, SALEMI B, et al. Modular self-reconfigurable robot systems [grand challenges of robotics][J]. *Robotics Automation Magazine*, 2007, 14(1): 2–11.

[10] RUS D, VONA M. Crystalline robots: Self-reconfiguration with compressible unit modules[J]. *Autonomous Robots*, 2001, 10(1): 107–124.

[11] SASTRA J, CHITTA S, YIM M. Dynamic rolling for a modular loop robot[J]. *The International Journal of Robotics Research*, 2009, 28(6): 758–773.

[12] BUTLER Z, RUS D. Distributed planning and control for modular robots with unit-compressible modules[J]. *The International Journal of Robotics Research*, 2003, 22(9): 699–715.

[13] BUTLER Z, FITCH R, RUS D. Distributed control for unit-compressible robots: goal-recognition, locomotion, and splitting[J]. *IEEE/ASME Transactions on Mechatronics*, 2002, 7(4): 418–430.

[14] SUH J W, HOMANS S B, YIM M. Telecubes: Mechanical design of a module for self-reconfigurable robotics[C]//*Proceedings of the IEEE International Conference on Robotics and Automation*, *ICRA*'02, Washington DC, USA, 2002, 4: 4095–4101.

[15] WELLER M P, KIRBY B T, BROWN H B, et al. Design of prismatic cube modules for convex corner traversal in 3D[C]//*IEEE/RSJ International Conference on Intelligent Robots and Systems*, St. Louis, USA, 2009: 1490–1495.

[16] KARAGOZLER M E, CAMPBELL J D, FEDDER G K, et al. Electrostatic latching for inter-module adhesion, power transfer, and communication in modular robots[C]//*IEEE/RSJ International Conference on Intelligent Robots and Systems*, San Diego, CA, USA, 2007: 2779–2786.

[17] YU C H, HALLER K, INGBER D, et al. Morpho: A self-deformable modular robot inspired by cellular structure[C] //*Proceedings of the IEEE International Conference on Robotics and Automation*, Nice, France, 2008: 3571–3578.

[18] YU C H, NAGPAL R. Self-adapting modular robotics: A generalized distributed consensus framework[C]//*Proceedings of the IEEE International Conference on Robotics and Automation*, Kobe, Japan, 2009: 1881–1888.

[19] UNSAL C, KHOSLA P K. Solutions for 3D self-reconfiguration in a modular robotic system: implementation and motion planning[C]//*Intelligent Systems and Smart Manufacturing. International Society for Optics and Photonics*, 2000: 388–401.

[20] PREVAS K C, UNSAL C, EFE M O, et al. A hierarchical motion planning strategy for a uniform self-reconfigurable modular robotic system[C]//*Proceedings of the IEEE International Conference on Robotics and Automation*, 2002, 1: 787–792.

[21] HJELLE D, LIPSON H. A robotically reconfigurable truss[C]// *ASME/IFToMM International Conference on Reconfigurable Mechanisms and Robots*, *IEEE*, 2009: 73–78.

[22] AN B K. EM-Cube: cube-shaped, self-reconfigurable robots sliding on structure surfaces[C]//*Proceedings of the IEEE International Conference on Robotics and Automation*, Pasadena, CA, USA, 2008: 3149–3155.

[23] MICHAEL J. *Fractal shape changing robot construction theory and application note*[M]. Robodyne Cybernetics Ltd, 1995.

[24] ROMANISHIN J W, GILPIN K, RUS D. M-blocks: Momentum-driven, magnetic modular robots[C]//*IEEE/RSJ International Conference on Intelligent Robots and Systems(IROS)*, *IEEE*, 2013: 4288–4295.

[25] AGRAWAL S K, KUMAR S, YIM M. Polyhedral single degree-of freedom expanding structures: design and prototypes[J]. *Transactions of the ASME*, *Journal of Mechanical Design*, 2002, 124(3): 473–478.

[26] CLARK P E, CURTIS S A, RILEE M L. A new paradigm for robotic rovers[J]. *Space, Propulsion & Energy Sciences International Forum*, 2001, 20: 308–318.

[27] CURTIS S A. ANTS as an architectural pathway to artificial life[R/OL]. *NASA Goddard Space Flight Center*, 2008, http://ants.gsfc.nasa.gov/index.html.

[28] DING W, YAO Y A. A novel deployable hexahedron mobile mechanism constructed by only prismatic joints[J]. *Transactions of the ASME*, *Journal of Mechanisms and Robotics*, 2013, 5(4): 041001–041016.

[29] HUANG Z. The kinematics and type synthesis of lower-mobility parallel manipulators[C]//*Proceedings of the 11th World Congress in Mechanism and Machine Science*, Tianjin, 2004: 65–76.

[30] GOGU G. Mobility of mechanisms: a critical review[J]. *Mechanism and Machine Theory*, 2005, 40(9): 1068–1097.

[31] HUANG Z, LIU J F, LI Q C. Unified methodology for mobility analysis based on screw theory[J]. *Smart Devices and Machines for Advanced Manufacturing*, Berlin: Springer-Verlag, 2008: 49–78.

[32] SUJAN V A, LICHTER M D, DUBOWSKY S. Lightweight hyper-redundant binary elements for planetary exploration robots[J].

Proceedings of the IEEE/ASME Conference on Advanced Intelligent Mechatronics, 2001, 2: 1273–1278.

[33] SUJAN V A, DUBOWSKY S. Design of a lightweight hyper-redundant deployable binary manipulator[J]. *Transactions of the ASME*, *Journal of Mechanical Design*, 2004, 126 (1): 29–39.

[34] MINOVIC P, ISHIKAWA S, KATO K. Symmetry identification of a 3-D object represented by octree[J]. *IEEE Transactions on Pattern Analysis and Machine Intelligence*, 1993, 15(5): 507–514.

[35] YIM M. *Locomotion with a unit-modular reconfigurable robot*[D]. Department of Mechanical Engineering, Stanford University, 1994.

[36] VUKOBRATOVIC M, FRANK A A, JURICIC D. On the stability of biped locomotion[J]. *IEEE Transactions on Biomedical Engineering*, 1970, 17(1): 25–36.

[37] VUKOBRATOVIC M, BOROVAC B. Dynamic balance concept and the maintenance of the dynamic balance in humanoid robotics[C]// *6th International Symposium on Intelligent Systems and Informatics*, Subotica, Serbia, 2008: 1–11.

[38] TAKNISHI A, TOCHIZAWA M, TAKEYA T, et al. Realization of dynamic biped walking stabilized with trunk motion under known external force[C]//*Proceedings of the International Conference on Advanced Robotics*, Columbus, USA, 1989: 323–330.

[39] LIU C H, LI R M, YAO Y A. An omnidirectional rolling 8U parallel mechanism[J]. *Transactions of the ASME, Journal of Mechanisms and Robotics*, 2012, 4(3): 034501–034506

Biographical notes

DING Wan, born in 1987, is current a PhD candidate at *School of Mechanical, Electronic and Control Engineering*, *Beijing Jiaotong University*, *China*. He received his bachelor degree from *Hubei Polytechnic University*, *China*, in 2009. His research interests include creative mechanism design and mobile robot.
Tel: +86-10-51685335; E-mail: dingwan@bjtu.edu.cn

WU Jianxu, born in 1989, is current a PhD candidate at *School of Mechanical, Electronic and Control Engineering*, *Beijing Jiaotong University*, *China*. He received his bachelor degree from *Taiyuan University of Science And Technology*, *China*, in 2012. His research interests include creative mechanism design and mobile robot.
Tel: +86-10-51685335; E-mail: 13116343@bjtu.edu.cn

YAO Yan'an, born in 1972, is current a professor and a PhD candidate supervisor at *School of Mechanical, Electronic and Control Engineering*, *Beijing Jiaotong University*, *China*. He received his bachelor degree from *Yanshan University*, *China*, in 1993. He received his master and PhD degree from *Tianjing University*, *China*, in 1999. He conducted research as a Postdoctorial Fellow at *Shanghai Jiaotong University* from1999 to 2001, and as a visitor at *RWTH Aachen Univeristy*, *Aachen*, *German*, during 2008 to 2009. His research interests include creative mechanism design and mobile robot.
Tel: +86-10-51685335; E-mail: yayao@bjtu.edu.cn